

Tracking Advanced Planetary Systems (TAPAS) with HARPS-N

II. Super Li-rich giant HD 107028^{★,★★,★★★}

M. Adamów^{1,2}, A. Niedzielski², E. Villaver³, A. Wolszczan^{4,5}, K. Kowalik⁶, G. Nowak^{7,8,2},
 M. Adamczyk², and B. Deka-Szymankiewicz²

¹ McDonald Observatory and Department of Astronomy, University of Texas at Austin, 2515 Speedway, Stop C1402, Austin, Texas, 78712-1206, USA

e-mail: madamow@astro.as.utexas.edu

² Toruń Centre for Astronomy, Faculty of Physics, Astronomy and Informatics, Nicolaus Copernicus University, Grudziadzka 5, 87-100, 87-100 Toruń, Poland

e-mail: Andrzej.Niedzielski@umk.pl

³ Departamento de Física Teórica, Universidad Autónoma de Madrid, Cantoblanco 28049 Madrid, Spain

e-mail: Eva.Villaver@uam.es

⁴ Department of Astronomy and Astrophysics, Pennsylvania State University, 525 Davey Laboratory, University Park, PA 16802, USA

e-mail: alex@astro.psu.edu

⁵ Center for Exoplanets and Habitable Worlds, Pennsylvania State University, 525 Davey Laboratory, University Park, PA 16802, USA

⁶ National Center for Supercomputing Applications, University of Illinois Urbana-Champaign, 1205 W Clark St, MC-257, Urbana, IL 61801, USA

⁷ Instituto de Astrofísica de Canarias, C/Vía Láctea, s/n, 38205 La Laguna, Tenerife, Spain

⁸ Departamento de Astrofísica, Universidad de La Laguna, 38206 La Laguna, Tenerife, Spain

Received 22 May 2015 / Accepted 9 July 2015

ABSTRACT

Context. Lithium-rich giant stars are rare objects. For some of them, Li enrichment exceeds the abundance of this element found in solar system meteorites, suggesting that these stars have gone through a Li enhancement process.

Aims. We identified a Li-rich giant HD 107028 with $A(\text{Li}) > 3.3$ in a sample of evolved stars observed within the PennState Toruń Planet Search. In this work we study different enhancement scenarios and we try to identify the one responsible for Li enrichment in HD 107028.

Methods. We collected high-resolution spectra with three different instruments, covering different spectral ranges. We determined stellar parameters and abundances of selected elements with both equivalent width measurements and analysis, and spectral synthesis. We also collected multi-epoch high-precision radial velocities in an attempt to detect a companion.

Results. Collected data show that HD 107028 is a star at the base of the red giant branch (RGB). Except for high Li abundance, we have not identified any other anomalies in its chemical composition, and there is no indication of a low-mass or stellar companion. We exclude Li production at the luminosity function bump on the RGB as the effective temperature and luminosity suggest that the evolutionary state is much earlier than the RGB bump. We also cannot confirm the Li enhancement by contamination as we do not observe any anomalies that are associated with this scenario.

Conclusions. After evaluating various scenarios of Li enhancement we conclude that the Li-overabundance of HD 107028 originates from main-sequence evolution, and may be caused by diffusion processes.

Key words. stars: individual: HD 107028 – stars: late-type – stars: fundamental parameters – stars: atmospheres – techniques: spectroscopic – planetary systems

1. Introduction

Lithium depletion is a natural prediction of stellar evolution. Not long after stars leave the main sequence they experience mixing called the first dredge-up (FDU) that will lower the surface abundance levels to values of $A(\text{Li}) = 1.5^1$ dex or less. However, about a hundred Li-rich stars ($A(\text{Li}) > 1.5$) among red giant (RG) stars have recently been found (Kumar et al. 2011, and references therein; Ruchti et al. 2011; Lebzelter et al. 2012; Martell & Shetrone 2013; Liu et al. 2014; Adamów et al. 2014).

Lithium enhancement via internal production on the red giant branch (RGB) can start at the earliest with the luminosity

¹ $A(\text{Li}) = \log \frac{n(\text{Li})}{n(\text{H})} + 12$.

* Based on observations obtained with the Hobby-Eberly Telescope, which is a joint project of the University of Texas at Austin, the Pennsylvania State University, Stanford University, Ludwig-Maximilians-Universität München, and Georg-August-Universität Göttingen.

** Based on observations made with the Italian Telescopio Nazionale Galileo (TNG) operated on the island of La Palma by the Fundación Galilei of the INAF (Istituto Nazionale di Astrofisica) at the Spanish Observatorio del Roque de los Muchachos of the Instituto de Astrofísica de Canarias.

*** Based on observations made with the Mercator Telescope, operated on the island of La Palma by the Flemish Community, at the Spanish Observatorio del Roque de los Muchachos of the Instituto de Astrofísica de Canarias.

function bump (LFB), shortly after the FDU ends. The LFB is a stage in RGB evolution for stars no more massive than $\approx 2.2 M_{\odot}$. It is associated with the removal of the molecular discontinuity that stems from FDU processes. During the LFB, a star takes a small “step-back” in its evolution on the Hertzsprung-Russell (HR) diagram - effective temperature increases, while luminosity decreases for a short time, and the stellar interior becomes turbulent (Eggleton et al. 2006). Lithium may be produced during this evolutionary phase via a Cameron-Fowler mechanism (Cameron & Fowler 1971) with the support of an extra-mixing mechanism. The Cameron-Fowler mechanism is probably responsible for Li production in stars on the asymptotic giant branch (AGB). In this case, thermal pulses can trigger non-convective mixing.

Additional mixing on the RGB begins at the LFB, and the so-called Li-flash is also believed to be associated with this phase (Charbonnel & Balachandran 2000; Pasquini et al. 2014). Thus, attempts to locate the Li-rich stars in the HR diagram have driven a number of studies trying to verify this Li-production mechanism (e.g., Brown et al. 1989; Pilachowski et al. 1988, 2000; Kumar et al. 2011; Ruchti et al. 2011; Lebzelter et al. 2012; Martell & Shetrone 2013). However, these studies have shown, that Li-rich stars can be found at different stages along the RGB evolution. Even more interesting, one of the most Li-rich stars, SDSS J0720+3036 with $A(\text{Li}) = 4.55 \pm 0.20$ (Martell & Shetrone 2013) was identified as a subgiant.

All the above has led to the proposal of a number of alternative mechanisms invoking the presence of an extra-mixing process or pollution scenarios to explain the high photospheric values. Thus, it has been argued that lithium could be enhanced as a consequence of the stellar readjustments following the accretion of substellar bodies (Alexander 1967; Siess & Livio 1999) or via the accretion of dense interstellar medium clouds whose chemical composition was altered by a nearby supernova explosions (Woosley & Weaver 1995). Lithium can also be externally delivered by a companion in a binary system if one of the components has already undergone lithium production on the AGB (Sackmann & Boothroyd 1999). All the scenarios based on external contamination, involve anomalies in chemical abundances other than Li, such as enhancement of neutron capture elements, that are produced via the *s*-process in evolved stars, or α and *r*-process elements, associated with supernovae (e.g., Terasawa et al. 2001). The accretion of substellar bodies should also increase stellar rotation (Carlberg et al. 2010, 2012) and may cause intense mass loss (de La Reza et al. 1997). The latest searches for planets around giants have provided an opportunity to study the possible connection between lithium abundance and hosting companions of different masses. A planetary companion was found to the Li-rich red giant BD+48 740 Adamów et al. (2012) and in a recent study done for a sample of giants observed within the PennState – Toruń Planet Search (PTPS) project, it was found that Li overabundance is in many cases associated with the presence of companions (Adamów et al. 2014).

All scenarios of Li enhancement on the RGB can potentially explain moderate Li overabundances ($A(\text{Li}) \lesssim 2.5$), but do not explain the existence of extremely lithium-rich stars. About a hundred lithium-rich giants have been discovered so far. About 14 of them are so-called super lithium-rich giant stars (Brown et al. 1989; Balachandran et al. 2000; Reddy & Lambert 2005; Carlberg et al. 2010; Kumar et al. 2011; Ruchti et al. 2011; Martell & Shetrone 2013; Monaco et al. 2014). These evolved stars have abundances exceeding the interstellar medium value, i.e., $A(\text{Li}) = 3.3$ (Asplund et al. 2009).

In this paper we report a chemical abundance analysis of the Li-rich giant star HD 107028. We found the star to have a $A(\text{Li})$ exceeding the value of 3.3 determined for meteorites. HD 107028 has also been the subject of a systematic search for a substellar companion using HARPS-N at the 3.6 m Telescopio Nazionale *Galileo* under our program TAPAS (Tracking Advanced Planetary Systems with HARPS-N) after it was shown that HET observations show radial velocity (RV) variation of 36 m s^{-1} , significantly larger than the expected stellar jitter.

The paper is organized as follows. In Sect. 2 we present the observations obtained for this target and we outline the reduction procedures. Sect. 3 presents stellar parameters. In Sect. 4 we present abundances determinations. Analysis of available RVs is discussed in Sect. 5. Section 6 presents data on mass loss and activity. Finally, Sect. 7, which includes the discussion and conclusions, closes the paper.

2. Observations and data reduction

HD 107028 (BD+69 657, HIP 59975) is a $V = 7.66$, $B - V = +0.84$, and $U - B = +0.45$ mag (Mermilliod 1986) G5 (Cannon & Pickering 1993) giant in Draco. New reduction of HIPPARCOS parallaxes delivers $\pi = 6.15 \pm 0.49$ mas and places the star at a distance of 163 pc (van Leeuwen 2007). One hundred and fifty-seven epochs of HIPPARCOS photometry reveal a constant light of $H_p = 7.8035 \pm 0.0013$ mag with a scatter of 0.015 mag. The star belongs to a sample of evolved stars observed within the PTPS project. Because of its strong Li lines and the RV variations that could not be resolved with HET precision, it was selected for the TAPAS project.

The spectroscopic observations presented in this paper were made with three instruments (see Table 1). The observation started with the 9.2 m effective aperture Hobby-Eberly Telescope (HET, Ramsey et al. 1998) and its High Resolution Spectrograph (HRS, Tull 1998) in the queue scheduled mode (Shetrone et al. 2007). We also observed HD 107028 with the 3.58 m Telescopio Nazionale *Galileo* (TNG) and its High Accuracy Radial Velocity Planet Searcher for the Northern hemisphere (HARPS-N, Cosentino et al. 2012) and with the 1.2 m *Mercator* telescope and Hermes spectrograph (Raskin et al. 2011). The instrumental setups, reduction, and radial velocity measurements for HET/HRS and TNG/HARPS-N were described in detail in Niedzielski et al. (2015; hereafter Paper I). We obtained a total of sixteen HET/HRS spectra with a typical signal-to-noise ratio (S/N) of 150–200 and 22 TNG/HARPS-N spectra with S/N of 30–100. We also obtained one HET/HRS spectrum made in a different than standard PTPS spectrograph configuration. This spectrum covers more red wavelength regions and includes CN lines at $\lambda 8003 \text{ \AA}$. We used standard IRAF scripts or HET/HRS data reduction. Data reduction for *Mercator*/Hermes spectrum was done using the automated pipeline.

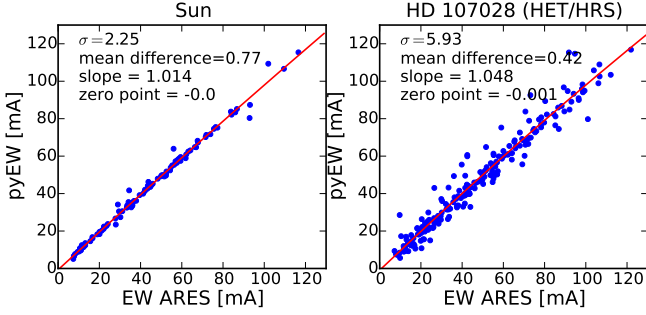
3. Stellar parameters

For the abundance analysis we used the four most suitable spectra available to us: two blue ones with the highest S/N, one from TNG/HARPS-N and the other from HRS/HRS (only in GC0 mode); and two red ones, a HET/HRS spectrum that covers the $\lambda 8000 \text{ \AA}$ region and one *Mercator*/Hermes spectrum.

The first estimate of stellar parameters was made using the available photometric data. For this purpose we used *BVJHK* magnitudes from TYCHO and 2MASS catalogs and T_{eff} – color calibrations from Ramírez & Meléndez (2005). From this analysis, the effective temperature of HD 107028 was estimated

Table 1. Spectroscopic material used in this work.

Instrument	Range	Resolution	S/N	Date
HET/HRS	4076–7838 Å	60 000	320 at 5936 Å	14 May 2006
HET/HRS	7109–10 917 Å	60 000	171 at 8991 Å	03 Mar. 2013
TNG/HARPS-N	3830–6930 Å	115 000	141 at 6582 Å	28 Apr. 2013
Mercator/Hermes	3770–9000 Å	85 000	178 at 7124 Å	22 Jan. 2015

**Fig. 1.** Comparison of equivalent widths determined with ARES and pyEW for the Sun and HD 107028.

as 5100 K but no reliable $\log g$ was available. The luminosity of HD 107028 was calculated from the HIPPARCOS parallax (van Leeuwen 2007).

To constrain the atmospheric parameters, mass, and luminosity of HD 107028 as well as possible, we repeated the analysis with new spectra and a new method. For this purpose, we developed a set of Python functions to measure equivalent widths (EWs) of Fe I and Fe II lines and to evaluate stellar parameters using the current version of the MOOG² stellar line analysis code (Snedden 1973).

The pyEW³ Python procedures for the determination of EWs is based on ideas used in the ARES code (Sousa et al. 2007). It redetermines the continuum in a small portion of the spectrum (usually 2 Å), calculates derivatives to detect positions of lines, and fits multiple Gaussian profiles to the observed spectrum. In Fig. 1 we present the comparison of equivalent widths determined with pyEW and ARES for the Sun (100 lines) using solar HARPS spectrum distributed with the ARES code, and for HD 107028 (208 lines). For the latter we used the HET/HRS spectrum. In both cases we obtained very good agreement, although the scatter, as expected, is higher for the HET/HRS spectrum given its lower S/N and resolution compared to the solar spectrum.

The analysis was done using three different spectra (the red HET/HRS was not included in the analysis) and two line sets. The first set of Fe I and II lines is from Takeda et al. (2005), who calibrated line data on the solar spectrum. The second set of neutral and ionized Fe and Ti features is a compilation of lines for which $\log gf$ are determined in laboratory studies. The $\log gf$ values for Fe I are taken from Den Hartog et al. (2014), Ruffoni et al. (2014), and O’Brian et al. (1991); the Fe II lines are from Meléndez & Barbuy (2009). We also added Ti I and Ti II lines with $\log gf$ values taken from Lawler et al. (2013) and Wood et al. (2013), respectively, obtained by the University of Wisconsin atomic physics group. From this compilation we chose isolated and moderately blended lines that are present in

our spectra. For the analysis we only used lines with equivalent widths in the $5 \text{ mÅ} < EW < 150 \text{ mÅ}$ range. We only used lines with $\lambda > 4350 \text{ Å}$ due to the low S/N on the blue end of all spectra of HD 107028.

In determining atmospheric parameters we used MOOG’s *abfind* driver executed from a python wrapper that iterates input stellar parameters and evaluates MOOG results. Iteration is made in the $(T_{\text{eff}}, \log g, v_{\text{mic}})$ space with the kMPFIT algorithm (a Python implementation of the Levenberg-Marquardt technique to solve the least-squares problem), which is a part of the Kapteyn package⁴. Adopted starting parameters are $T_{\text{eff}} = 5100 \text{ K}$ (obtained from photometric data), $\log g = 3.0$, $v_{\text{mic}} = 1.0 \text{ km s}^{-1}$, and $[\text{Fe}/\text{H}] = 0.0$. For the calculations, we used a grid of atmospheres by Castelli & Kurucz (2004). For a given set of T_{eff} , $\log g$, v_{mic} , and $[\text{Fe}/\text{H}]$, we update the atmosphere model using a tool by Andy McWilliam and Inese Ivans for interpolating between grids. During every iteration, all abundances for single Fe I and Fe II lines that differ from the average Fe I and Fe II values (respectively) by more than 1σ are removed from the fit. This criterion might be considered too strict, but initial σ is calculated for all abundances from all automatically measured lines. Usually, there are some faulty EW measurements among them that need to be removed from further analysis. In the case of HD 107028, a 1σ threshold means eliminating all values for which the difference between a single abundance and the average abundance is greater than 0.5 dex. The input file where the lines and their EWs are listed is not edited and so this procedure is repeated for every iteration.

The results obtained for different line lists and stellar spectra are summarized in Table 2. Uncertainties presented there are estimated in a way proposed by Gonzalez & Vanture (1998). The uncertainties in T_{eff} and v_{mic} were estimated based on parameters of abundances versus excitation potential and reduced EWs fits, respectively, for the best model. Uncertainty in $\log g$ is a quadrature sum of the uncertainty in T_{eff} and the scatter in Fe II abundances, and for uncertainty in $[\text{Fe}/\text{H}]$ is a quadrature sum of the uncertainties in T_{eff} , $\log g$, v_{mic} , and the scatter in Fe I abundances.

The final parameters adopted for further analysis are $T_{\text{eff}} = 5133 \pm 53 \text{ K}$, $\log g = 2.97 \pm 0.09$, $v_{\text{mic}} = 1.08 \pm 0.08 \text{ km s}^{-1}$, and $[\text{Fe}/\text{H}] = -0.28 \pm 0.08$ (averaged values). The effective temperature we obtained is in agreement with the one based on intrinsic colors. These parameters unambiguously locate HD 107028 in the subgiants/giants area in the HR diagram.

The stellar mass and age of HD 1070028 were estimated on the basis of spectroscopically determined atmospheric parameters through the construction of a probability distribution function using an estimation by da Silva et al. (2006) and stellar isochrones from PARSEC (PAdova and TRIeste Stellar Evolution Code, Bressan et al. 2012). The stellar radius was estimated from the derived masses and $\log g$ values obtained

² <http://www.as.utexas.edu/~chris/moog.html>

³ <https://github.com/madamow/pyEW>

⁴ <https://www.astro.rug.nl/software/kapteyn/index.html>

Table 2. Summary of parameters for HD 107028 and Sun.

Fe lines by Takeda				
Parameter	HET/HRS	HERMES	HARPS-N	Sun
T_{eff} [K]	5124 ± 41	5109 ± 38	5104 ± 39	5790 ± 47
$\log g$	2.97 ± 0.06	3.01 ± 0.06	3.0 ± 0.06	4.44 ± 0.06
v_{mic} [km s ⁻¹]	1.05 ± 0.06	1.11 ± 0.05	1.03 ± 0.06	0.97 ± 0.06
[Fe/H]	-0.25 ± 0.06	-0.30 ± 0.05	-0.26 ± 0.06	-0.09 ± 0.06
EP slope	0.00238	0.00706	-0.00308	-0.01773
RW slope	0.00121	-0.00465	-0.04525	0.02918
n_{FeI}	194	227	193	173
n_{FeII}	15	18	14	14
Compilation of Fe and Ti lines with laboratory data				
Parameter	HET/HRS	HERMES	HARPS-N	Sun
T_{eff} [K]	5190 ± 70	5139 ± 67	5132 ± 64	5833 ± 63
$\log g$	2.96 ± 0.11	2.94 ± 0.11	2.94 ± 0.11	4.37 ± 0.13
v_{mic} [km s ⁻¹]	1.19 ± 0.10	1.07 ± 0.09	1.04 ± 0.09	0.96 ± 0.08
[Fe/H]	-0.32 ± 0.10	-0.31 ± 0.10	-0.23 ± 0.09	-0.03 ± 0.08
EP slope	0.01685	-0.00414	0.00675	-0.00641
RW slope	-0.025578	-0.00981	-0.02349	0.02659
n_{FeI}	78	103	96	96
n_{FeII}	33	38	31	33

Table 3. Summary of available data on HD 107028.

Parameter	Value	Reference
V [mag]	7.57	ESA (1997)
$B - V$ [mag]	0.84	Mermilliod (1986)
π [mas]	6.15 ± 0.49	van Leeuwen (2007)
$(B - V)_0$ [mag]	0.816	
M_V [mag]	1.54	
T_{eff} [K]	5133 ± 53	This work
$\log g$	2.97 ± 0.09	This work
[Fe/H]	-0.28 ± 0.08	This work
v_{mic} [km s ⁻¹]	1.08 ± 0.08	This work
RV [km s ⁻¹]	-24.985 ± 0.026	Nowak (2012)
$v_{\text{rot}} \sin i_{\star}$ [km s ⁻¹]	1.46 ± 1.19	Adamów (2014)
M/M_{\odot}	1.72 ± 0.21	This work
$\log L/L_{\odot}$	1.37 ± 0.12	This work
R/R_{\odot}	6.6 ± 1.0	This work
$\log \text{age}$	9.20 ± 0.14	This work
V_{osc} [m s ⁻¹]	3.01	This work
P_{osc} [d]	0.07	

from the spectroscopic analysis, and using the derived luminosities and effective temperatures. The adopted radius is the average of the two estimates. The $v_{\text{rot}} \sin i_{\star}$ was obtained via SME (Valenti & Piskunov 1996) by modeling a set of spectral lines with a procedure described by Adamów et al. (2014). The stellar parameters of HD 107028 are summarized in Table 3 and its location on the Hertzsprung-Russell diagram is presented in Fig. 2.

4. Abundances

Lithium, CNO, neutron capture elements abundances, and carbon isotopic ratio analysis was performed with a Python code that make use of the MOOG code (*synth* driver). The use of spectral synthesis techniques in obtaining abundances of those

elements is motivated by the fact that their lines are blended with other structures, they might be affected by telluric lines, or – as in the case of C and N – the abundance analysis is based on molecular lines. The procedure starts by building an initial synthetic spectrum that is then cross correlated with the observations to determine possible RV shifts. After that, an automatic abundance analysis is performed where fitting a requested set of chosen free parameters is executed using the kMPFIT algorithm. Except for abundances, we look for the best value of a parameter that describes Gaussian smoothing of a synthetic spectrum and we allow for small adjustments of the continuum level. In this iterated procedure, new synthetic spectra with a varying set of abundances is compared to the observed spectra in search of the best fit.

We determined abundances of the α elements using the isolated lines selected by Ramírez & Allende Prieto (2011) from the measurement of their equivalent widths. Our final abundances for HD 107028 are summarized in Table 4.

4.1. Lithium

The Li I 6708 Å resonance feature is one of the strongest lines in HD 107028 spectra and proves that this star should be classified as a Li-rich giant (see also Fig. 3 for lithium abundance distribution for evolved stars from the PTPS sample).

The subordinate 6104 Å line is also detectable in this star, but it is much weaker and is located near strong Fe structures. Lithium abundance for HD 107028 was determined using the two lines from the TNG/HARPS-N spectrum with the best S/N (141 around 6708 Å and 152 close to 6103 Å). The obtained values, presented in Table 4, are in agreement; however, the abundance based on the stronger, redder line might be underestimated as the model spectrum does not reach the core of the spectral line (Fig. 4, middle panel). In the case of HD 107028, the imperfect fit of the bottom of the line may be caused by the fact that models might not properly consider the environment where the 6708 Å line is formed. This difference in abundances derived from the two Li lines

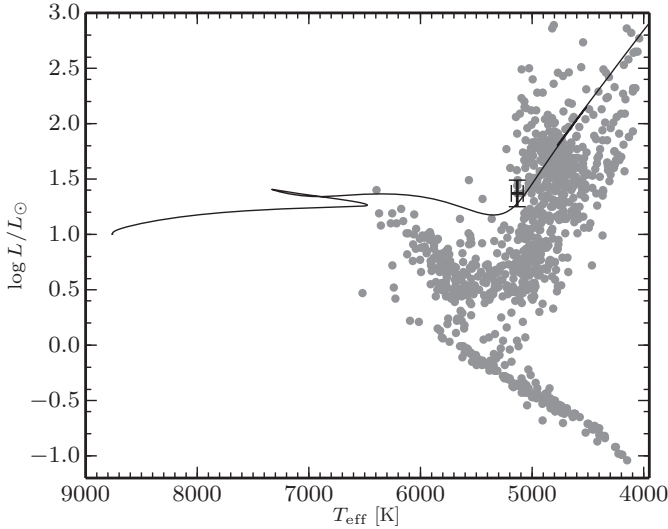


Fig. 2. HD 107028 on top of all PTPS stars. The evolutionary track comes from PARSEC and it starts with hydrogen ignition.

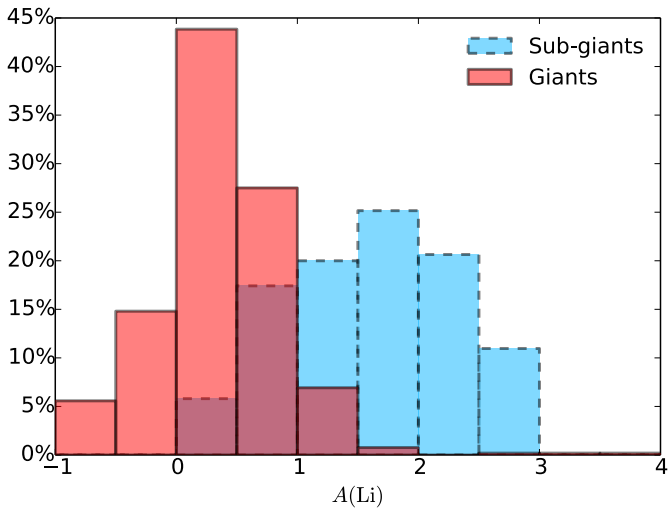


Fig. 3. Distribution of Li abundances for evolved stars observed within PTPS (Adamów 2014).

is also observed for other Li-rich giants, i.e., for those discussed in Martell & Shetrone (2013). Lithium lines may be subject to several non-LTE processes (Carlsson et al. 1994, and references therein). We applied the non-LTE corrections provided by Lind et al. (2009) to our LTE lithium abundances, calculated for a star of given T_{eff} , $\log g$, v_{mic} , and $[\text{Fe}/\text{H}]$.

The *Mercator*/Hermes spectrum also includes red Li lines at 8126 Å. These lines are blended with Fe and CN structures and are located in a region of the spectrum that may be affected by H₂O telluric bands. Telluric correction has not been applied to the *Mercator*/Hermes spectrum, but, based on the plot of the spectrum in Fig. 4 (lower panel) where the best fit of the stellar synthetic spectrum to the observational data is presented, there is no significant telluric contamination close to the Li line that could influence the abundance determination. The obtained value of $A(\text{Li})$ of 3.64 is in good agreement with the value determined from the $\lambda 6103$ Å line.

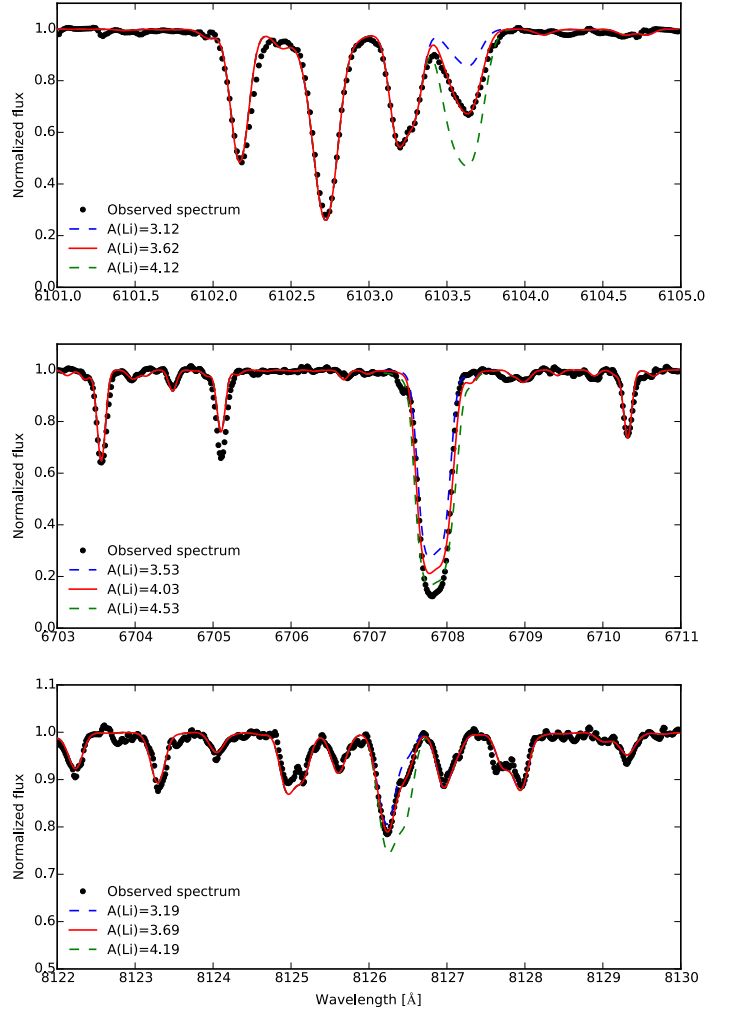


Fig. 4. Lithium lines identified in the HD 107028 spectrum.

4.2. CNO abundances and carbon isotopic ratio

The oxygen abundance was obtained from the analysis of the lines at $\lambda 6300$ and 6363 Å. Since these two lines are not affected by non-LTE effects, no non-LTE correction was applied to determine the oxygen abundance. Both lines lie in a region affected by telluric lines, hence spectral analysis was performed on a spectrum to which telluric division had been applied. The line at $\lambda 6300$ Å is also blended with a Ni line and lies in region where CN bands may influence the analysis.

The oxygen abundance was also obtained from the analysis of the $\lambda 7772$, 7774 , 7775 Å triplet, available from the HET/HRS and *Mercator*/Hermes spectra. Since the oxygen triplet is strongly affected by non-LTE effects, we applied the empirical non-LTE corrections by Afşar et al. (2012).

Carbon abundance was determined by modeling several C₂ (near 5160 Å and 5635 Å) and CH bands (4230 – 4240 Å and 4300 – 4325 Å). The abundance of carbon obtained is $[\text{C}/\text{H}] = -0.50 \pm 0.05$.

The abundance of nitrogen was determined based on CN bands near 8003 Å using the red HET/HRS spectrum and the *Mercator*/Hermes spectrum. Although the HET/HRS spectrum has a low S/N, the values measured from both spectra are in agreement. Nitrogen, with an abundance of $[\text{N}/\text{H}] = 0.6$, is enhanced in the HD 107028 atmosphere. However, it is important to keep in mind that the N abundance determined using

CN bands strongly depends on the C abundance introduced in the analysis.

The *Mercator*/Hermes spectrum, which targets CN bands at 8003 Å, was used to determine the carbon isotopic ratio. The ^{13}C lines are visible but they are not strong, and the obtained $^{12}\text{C}/^{13}\text{C}$ ratio is 25. The S/N covering the CN bands close to 8003 Å is too low to determine a reliable $^{12}\text{C}/^{13}\text{C}$ carbon isotopic ratio using the HET/HRS spectrum and so for this purpose we used the CH bands near 4230 and 4370 Å and compared the observational data with a synthetic spectra using MOOG assuming different carbon isotopic ratios. The determinations based on different molecules are in agreement, showing that in HD 107028 the FDU is in progress. Line data for C_2 comes from Ram et al. (2014) and Brooke et al. (2013), CN and CH data were taken from Sneden et al. (2014) and Plez & Cohen (2005), respectively.

4.3. Abundances of α -group, neutron capture elements, and kinematics

The α element abundances were measured using EWs for several Na, Mg, Al, Ca, Ti, and Ni lines selected from Ramírez & Allende Prieto (2011) and using their line data. The EWs were obtained automatically with pyEW by fitting Gaussian profiles to selected lines using the *Mercator*/HERMES spectrum. Abundances were obtained using MOOG's *abfind* driver.

To determine the abundances of neutron capture elements we used the Ba II line at $\lambda 6141$ Å, two La II lines at $\lambda 6262$ and $\lambda 6390$ Å, and one Eu II line at $\lambda 6645$ Å. All these lines have complex structures with isotopic and hyperfine splitting; therefore, we used spectral synthesis to analyze them. Line data for these transitions were taken from Lawler et al. (2001a,b). Strontium abundance was calculated using line at $\lambda 4077.71$ Å. All derived abundances for those elements are shown in Table 4 and they are consistent with the abundances of nearby giants of similar metallicity (see, e.g., Luck & Heiter 2007 and Afşar et al. 2012).

The overall results of our abundance analysis are presented in Table 4. For HD 107028 we find typical values of a thin-disk, subsolar metallicity star, and to check its consistency we also computed space velocity components (U, V, W) following Johnson & Soderblom (1987), but using the J2000 epoch in the coordinates and the transformation matrix, and parallax and proper motions from the Tycho/HIPPARCOS Catalog (van Leeuwen 2007). We obtain spatial velocities (U, V, W) = (−87, −59, −51) km s $^{-1}$ and the distance to the galactic plane $z = 0.13$ kpc. Hence, according to the Ibukiyama & Arimoto (2002) criteria, HD 107028 is a member of the galactic thin disk population. This result agrees with the chemical composition of this star, typical for an object from the galactic thin disk.

5. Radial velocities

HD 107028 was observed within PTPS at 15 epochs over 2669 days between MJD = 53 755.47 and 56 425.15 (Table 5). It showed low-level RV variations of 36 m s $^{-1}$ with average uncertainty of 6 m s $^{-1}$ (i.e., 6σ). The RV variability was found to be over an order of magnitude larger than the expected amplitude of p-mode oscillations. We also observed bisector (BS) variations of 82 m s $^{-1}$ with an average uncertainty of 16 m s $^{-1}$ and of unclear nature, but uncorrelated with the RV ($r = -0.03$). No periodic signal was found in these data. A cross-correlation analysis of line profiles in the HET/HRS blue CCD GC0 spectrum of

Table 4. Summary of abundances on for HD 107028.

Element	$A(X)_{\text{LTE}} \pm \sigma$	$A(X)_{\text{NLTE}}$	$A(X)_{\odot}$	[X/H]	[X/Fe]
Li _{6104 Å}	3.62	3.73	1.05		
Li _{6708 Å}	4.03	3.54	1.05		
Li _{8126 Å}	3.69		1.05		
C	7.93 ± 0.05		8.43	−0.50	−0.23
N	8.22		7.83	0.39	0.66
O	8.47 ± 0.02		8.69	−0.22	0.05
α elements					
Mg	7.55 ± 0.15		7.60	−0.05	0.22
Si	7.36 ± 0.06		7.51	−0.15	0.12
Ca	6.20 ± 0.07		6.34	−0.14	0.13
Ti	4.75 ± 0.09		4.95	−0.20	0.07
Neutron-capture elements					
Sr II	2.49		2.87	−0.38	−0.11
Ba II	2.12		2.18	−0.06	0.21
La II	0.74 ± 0.17		1.10	−0.36	0.17
Eu II	0.34		0.52	−0.18	0.09
Other elements					
Na	6.19 ± 0.05		6.24	−0.05	0.22
Al	6.35 ± 0.07		6.45	−0.10	0.17
Ni	6.15 ± 0.08		6.22	−0.07	0.20

Notes. Errors on $A(X)$ are standard deviations and they cover line-to-line deviations only.

HD 107028 (unaffected by I_2 lines), as well as its GC1 spectra (cleaned from I_2 lines in the process of radial velocity measurements, Nowak 2012; Nowak et al. 2013) showed a regular shape for the cross-correlation function and no trace of a companion.

We attempted to resolve this variability with the more precise and stable TNG/HARPS-N instrument given that following e.g., Adamów et al. (2014), Li-overabundance in giants seems to be related to the presence of companions. After 21 epochs of observations with TNG/HARPS-N taken over 517 days between MJD = 56 277.26 and 56 795.04 we found RV variations of only 22 m s $^{-1}$ with average uncertainty of 1.2 m s $^{-1}$ and uncorrelated ($r = -0.19$) BS variations of only 10 m s $^{-1}$ (Table 6). Neither of these data sets alone, or combined with HET, showed a periodic signal. Our hybrid approach to model the data (see Paper I for details) also failed.

With RV measurements only, we cannot definitely exclude that this star hosts a companion, as the orbital inclination of the potential companions may be such that $\sin i \approx 0$. This kind of “pole-on” systems are not detectable in radial velocity searches. However, the low level of observed RV variations, with an amplitude of only 22 m s $^{-1}$, the lack of correlation between RV and BS, and the regular shape of the cross-correlation function suggests that it is better to consider HD 107028 a single star. The mean absolute RV of HD 107028 is -24.485 ± 0.007 km s $^{-1}$.

This radial velocity differs from an earlier measurement (-29.20 ± 1.2 km s $^{-1}$; Wilson 1953) by ~ 4.7 km s $^{-1}$. This point cannot be included in RV fitting for several reasons: there is no date and time when this RV measurement was done, the precision of measurements is very different, and finally the time separation between Wilson's measurements and ours is more than 55 years. All of this leads to unambiguous orbital solutions, but may suggest that HD 107028 has a low-mass companion on a highly elliptical, long-period orbit.

Table 5. HET and HRS measurements of HD 107028.

MJD	RV	σ_{RV}	BS	σ_{BS}
53 755.475041	-18.19	6.53	-4.74	17.59
53 808.329433	-10.37	4.84	24.00	16.14
53 843.191794	-2.36	4.35	63.56	10.59
53 893.124855	-8.02	6.54	-18.12	11.80
54 463.522598	-14.36	6.64	7.16	21.12
54 520.372234	-12.07	6.02	49.32	9.85
56 288.509421	-2.34	6.88	45.15	22.29
56 308.463090	-7.34	5.80	26.25	15.41
56 323.433646	8.92	5.57	-1.68	14.49
56 335.412303	13.11	6.21	47.18	19.64
56 354.352824	9.55	5.64	0.42	17.89
56 367.318287	17.31	6.30	-10.13	17.01
56 379.282778	9.95	5.29	4.65	15.76
56 395.245718	9.07	5.77	33.99	16.49
56 425.153495	4.00	5.89	43.69	15.70

Notes. Radial velocity (RV), bisector (BS), and their respective errors are measured in m s^{-1} .

Table 6. TNG and HARPS-N measurements of HD 107028.

MJD	RV	σ_{RV}	BS
56 277.260735	-24495.51	0.81	35.19
56 294.242058	-24488.44	0.71	35.85
56 321.142563	-24481.60	1.00	42.60
56 374.005509	-24493.47	0.74	33.45
56 410.913816	-24475.76	0.63	36.11
56 411.009163	-24492.93	0.68	33.82
56 430.967926	-24486.64	0.83	38.61
56 469.876485	-24490.62	1.31	38.47
56 469.959043	-24490.51	1.59	32.90
56 647.252802	-24492.09	1.83	41.94
56 685.115550	-24475.23	1.23	32.95
56 685.213074	-24473.66	1.30	33.72
56 685.275789	-24475.27	1.61	32.89
56 739.967323	-24488.57	1.08	42.47
56 740.025788	-24491.21	1.27	39.73
56 740.101594	-24486.80	1.63	41.03
56 740.142011	-24488.17	1.15	41.92
56 770.022102	-24487.05	1.02	38.44
56 770.070215	-24486.01	0.96	36.24
56 794.901061	-24473.29	1.29	38.94
56 795.040834	-24480.07	1.92	35.49

Notes. Radial velocity (RV), its error, and bisector (BS) are measured in m s^{-1} .

We cannot definitely exclude the possibility that our observations cover only the flat part of the RV curve during one orbital period. However, assuming that the amplitude in RVs should be close to 5 km s^{-1} and that we have observed only a flat fragment of the RV curve, the orbit of the companion hosted by HD 107028 should have $e \gtrsim 0.8$ and a very specific orientation in space (longitude of ascending node of 0° or 180°). In any other cases, a long-term trend in RVs should be easily detected in TNG/HARPS or HET/HRS data, but we did not observe it.

Therefore, collected observations cannot definitely exclude the hypothesis that HD 107028 hosts a companion on an elliptical orbit and one needs to keep in mind that RV technique effectiveness depends on system orientation in space. However, we

claim that the presence of such a companion is unlikely, as we do not see any long-term trends in collected RV data. We also argue that the radial velocity measurement by Wilson (1953) might be overestimated for HD 107028.

6. Line profile variations: activity and traces of mass loss

The Ca II H & K line profiles are widely accepted as stellar activity indicators. Both the Ca II H & K lines and the infrared Ca II triplet lines at $8498\text{--}8542 \text{ \AA}$ lay outside the HET/HRS wavelength range, but the Ca II H & K lines are available to us in the TNG HARPS-N spectra and the $8498\text{--}8542 \text{ \AA}$ range is present in the *Mercator*/Hermes spectrum. Although the S/N in the blue spectrum for this red giant is not high, no trace of the reversal that is typical for active stars (Eberhard & Schwarzschild 1913) is present, and no obvious chromospheric activity can be demonstrated either for the TNG/HARPS-N or for the *Mercator*/Hermes spectra. To quantify possible activity-induced line profile variations, we calculated the S_{HK} index according to the Duncan et al. (1991) prescription for all 21 epochs of HARPS-N observations. The mean value is $S_{HK} = 0.35 \pm 0.02$, which places HD 107028 among moderately active subgiants according to Isaacson & Fischer (2010).

One of the explanations for Li overabundances in evolved stars implies that Li enhancement is associated with mass ejections (in the form of dust) from the star (see, e.g., de La Reza et al. 1997; Siess & Livio 1999; Bharat Kumar et al. 2015) that we would see as infrared excesses. To verify whether HD 107028 presents an infrared excess, we queried the WISE (Wright et al. 2010) and 2MASS catalogs. The brightness of the star in $K\text{-WISE}[12 \mu\text{m}]$ and $J - K$ 2MASS colors seems to be rather typical when compared to larger samples, like those presented by Lebzelter et al. (2012) or Adamów et al. (2014). Hence, we cannot report a significant infrared excess for HD 107028.

If the star has an intensive mass-loss in the form of gas, it should be reflected in the spectral line shape. Reddy et al. (2002) has shown that this phenomena might be observed through the Na D line profiles – an additional component to the sodium doublet should be present in the blue wing of stellar sodium lines. Again, we have not observed any irregularities of Na D lines or additional components to them. Therefore, HD 107028 does not seem to have gone through an intensive mass loss episode recently, either in the form of dust or gas.

7. Discussion

HD 107028 is a giant of $1.7 M_\odot$ that has recently started its evolution on the RGB. Its combination of effective temperature, surface gravity, and $^{12}\text{C}/^{13}\text{C}$ is consistent with a star that has already started the FDU and passed the point where Li depletion starts and carbon isotopic ratio drops (Charbonnel & Balachandran 2000). Our derived $^{12}\text{C}/^{13}\text{C} \sim 25$ value is in agreement with the value obtained by Sweigart et al. (1989) for a star with T_{eff} , $\log L/L_\odot$, and $[\text{Fe}/\text{H}]$ similar to those determined for HD 107028.

The prominent lithium overabundance for HD 107028, $A(\text{Li}) \geq 3.6$, places the star among the most Li-rich stars known and cannot be explained with Li production mechanisms at the LFB because this star has not reached this phase yet, even if we assume the low-mass star evolution model proposed by

Denissenkov (2012) where LFB occurs for lower effective temperatures (~ 5000 K).

Stars with high Li abundance that are still undergoing FDU can be misidentified as Li-rich giants. These are intermediate-mass stars that leave the MS with relatively high Li abundance; at the bottom of the RGB they may still have $A(\text{Li}) \approx 1.5$, which is usually adopted as a lower limit for considering a star Li rich. The lithium abundance observed in HD 107028 is higher than the value expected for population I stars on the MS ($A(\text{Li}) = 3.3$), even though this star has partially gone through the FDU process. Therefore, the chemical composition of HD 107028 must have been modified by some Li enhancement process.

The first dredge-up is the only known process that can alter the chemical composition of single stars during the subgiant evolution, but it does not result in Li (or any other element) production. Hence, the observed high Li abundance in HD 107028 might have originated during the MS evolution of the star. There are several other stars that reveal high Li abundance and have not reach the RGB yet. Three of them are turn-off stars located in clusters (Deliyannis et al. 2002; Koch et al. 2012; Monaco et al. 2012) and the fourth is a field subgiant detected by Martell & Shetrone (2013).

External pollution is an alternative to lithium nucleosynthesis in the stellar interior, and it is expected to be associated with enhancements in the α group and neutron-capture elements. This, however, does not seem to be the case in HD 107028 since the Li overabundance is not associated with α group or neutron capture elements enrichment, all of which have typical values of a thin-disk star with metallicity of -0.3 .

Exoplanet observations show a lack of close planets ($a < 0.6$ AU) around evolved stars for which planetary engulfment is a very plausible explanation (see, e.g., Villaver & Livio 2009; Villaver et al. 2014).

In principle, HD 107028 is evolved enough to have been able to ingest a hypothetical inner companion, assuming that its orbit was close enough. In known hot Jupiter systems, the semimajor axis is usually smaller than 0.05 AU (the stellar radius for HD 107028 is $6.6 R_{\odot} \approx 0.03$ AU).

However, we find it very unlikely that planet engulfment has a strong influence on the Li enrichment found in HD 107028. First of all, the HD 107028 Li abundance is too high. In order to raise the stellar Li abundance to a $A(\text{Li}) = 3.6$ level, an unrealistic number of planets needs to be engulfed (a few hundred Jupiter-like objects). Their chemical composition must be peculiar, i.e., their lithium abundance must exceed the value observed for the interstellar medium (assuming the model for Li enhancement via engulfment discussed by Carlberg et al. 2012). Moreover, the presence of an external companion as the cause (or effect via dynamical interactions within a system that might have caused ingestion) of the anomalous Li measurement is unlikely because precise radial velocity measurements obtained within the PTPS and TAPAS projects do not show any periodic signal that might be interpreted as a low-mass companion. We do not find any other signs of phenomena that could be associated with an engulfment episode. HD 107028 is a slow rotator with $v_{\text{rot}} \sin i_{\star} = 1.5 \text{ km s}^{-1}$, which is typical for an evolved star, but it is also consistent with a pole-on rotating star. It also shows no signs of enhanced mass loss, either in the form of gas or dust.

Contamination from more evolved stellar companions was suggested as the most likely explanation for the high Li abundance measured for the Li-rich objects located in the NGC 6397 (Koch et al. 2012) and M 4 (Monaco et al. 2012) clusters. This scenario cannot be applied to account for the Li abundance found

in HD 107028 as we do not find any signs of companions in the radial velocity measurements.

Deliyannis et al. (2002) proposed diffusion as a process leading to Li overabundance in the turn-off star J37 in the NGC 6633 cluster. For this star Li overabundance is not the only observed anomaly in the chemical composition. Even though kinematic data and photometry locate J37 as a member of NGC 6633, its Fe abundance is significantly higher (2–3 times) than for the rest of the stars assigned to the cluster. Elements like Ni, S, Si, Ca, and Al are also enriched, while C is depleted. Diffusion is a process that can explain a so-called Li-dip (or Li-gap) a sudden drop in Li abundances for MS stars in a specified effective temperature range. However, on the hot side of the Li-dip, the diffusion model predicts Li enhancement. In this narrow range of effective temperatures, the Li abundance can be raised to the level of $A(\text{Li}) \approx 4.7$ (see Fig. 2 in Deliyannis et al. 2002).

If we trace back the evolution of HD 107028 as a $1.7 M_{\odot}$ star to the MS (we do not expect intensive mass loss between the MS and its current location on the HR diagram as we do not see any signs of it in the data), we find that its effective temperature on the MS was in the range from ~ 8900 K to ~ 6500 K (see Fig. 2). This means that HD 107028 can fit into the diffusion model presented in Deliyannis et al. (2002). It is hard to say whether the chemical composition of HD 107028 differs from other stars (with the exception of Li) as this kind of comparison is more difficult for a field object from the galactic disk than for a member of the stellar cluster. Nevertheless, based on $[\text{Fe}/\text{H}]$ vs. $[\text{X}/\text{H}]$ trends for stars in the galactic disk, HD 107028 should be considered a typical star rather than an outsider. The chemical composition of HD 107028 was altered by some extraordinary event or process, and for some reason this unknown process does not affect other elements as remarkably as it does Li.

In this work we have shown that the nature of Li enhancement in HD 107028 is not connected to Li production on the RGB or to contamination scenarios. However, this object is a very interesting case for studying Li processing in stars.

Acknowledgements. We thank the HET and IAC resident astronomers and telescope operators for their support. We would like to thank Dr. Sergio Simon Diaz from IAC for obtaining the *Mercator/Hermes* spectrum used in this work. We also thank Dr. Christopher Sneden for comments that greatly improved the manuscript. M.A. acknowledges the Mobility+III fellowship from the Polish Ministry of Science and Higher Education. M.A., A.N., B.D. and M.A. were supported by the Polish National Science Centre grant No. UMO-2012/07/B/ST9/04415. E.V. acknowledges support from the Spanish Ministerio de Economía y Competitividad under grant AYA2013-45347P. K.K. was funded in part by the Gordon and Betty Moore Foundation's Data-Driven Discovery Initiative through Grant GBMF4561. This research was supported in part by PL-Grid Infrastructure. The HET is a joint project of the University of Texas at Austin, the Pennsylvania State University, Stanford University, Ludwig-Maximilians-Universität München, and Georg-August-Universität Göttingen. The HET is named in honor of its principal benefactors, William P. Hobby and Robert E. Eberly. The Center for Exoplanets and Habitable Worlds is supported by the Pennsylvania State University, the Eberly College of Science, and the Pennsylvania Space Grant Consortium. This work is based on observations obtained with the HERMES spectrograph, which is supported by the Fund for Scientific Research of Flanders (FWO), Belgium, the Research Council of K.U.Leuven, Belgium, the Fonds National de la Recherche Scientifique (F.R.S.-FNRS), Belgium, the Royal Observatory of Belgium, the Observatoire de Genève, Switzerland and the Thüringer Landessternwarte Tautenburg, Germany. This work makes use of Astropy, a community-developed core Python package for Astronomy, as well as SciPy and NumPy.

References

- Adamów, M. 2014, Ph.D. Thesis, UMK Toruń
- Adamów, M., Niedzielski, A., Villaver, E., Nowak, G., & Wolszczan, A. 2012, *ApJ*, 754, L15

- Adamów, M., Niedzielski, A., Villaver, E., Wolszczan, A., & Nowak, G. 2014, *A&A*, **569**, A55
- Afşar, M., Sneden, C., & For, B.-Q. 2012, *AJ*, **144**, 20
- Alexander, J. B. 1967, *The Observatory*, **87**, 238
- Asplund, M., Grevesse, N., Sauval, A. J., & Scott, P. 2009, *ARA&A*, **47**, 481
- Balachandran, S. C., Fekel, F. C., Henry, G. W., & Uitenbroek, H. 2000, *ApJ*, **542**, 978
- Bharat Kumar, Y., Reddy, B. E., Muthumariappan, C., & Zhao, G. 2015, *A&A*, **577**, A10
- Bressan, A., Marigo, P., Girardi, L., et al. 2012, *MNRAS*, **427**, 127
- Brooke, J. S. A., Bernath, P. F., Schmidt, T. W., & Bacskey, G. B. 2013, *J. Quant. Spectr. Rad. Transf.*, **124**, 11
- Brown, J. A., Sneden, C., Lambert, D. L., & Dutchover, Jr., E. 1989, *ApJS*, **71**, 293
- Cameron, A. G. W., & Fowler, W. A. 1971, *ApJ*, **164**, 111
- Cannon, A. J., & Pickering, E. C. 1993, *VizieR Online Data Catalog*: III/135
- Carlberg, J. K., Smith, V. V., Cunha, K., Majewski, S. R., & Rood, R. T. 2010, *ApJ*, **723**, L103
- Carlberg, J. K., Cunha, K., Smith, V. V., & Majewski, S. R. 2012, *ApJ*, **757**, 109
- Carlsson, M., Rutten, R. J., Bruls, J. H. M. J., & Shchukina, N. G. 1994, *A&A*, **288**, 860
- Castelli, F., & Kurucz, R. L. 2004, *IAU Symp.*, **210**, poster A20
- Charbonnel, C., & Balachandran, S. C. 2000, *A&A*, **359**, 563
- Cosentino, R., Lovis, C., Pepe, F., et al. 2012, in SPIE Conf. Ser., 8446
- da Silva, L., Girardi, L., Pasquini, L., et al. 2006, *A&A*, **458**, 609
- de La Reza, R., Drake, N. A., da Silva, L., Torres, C. A. O., & Martin, E. L. 1997, *ApJ*, **482**, L77
- Deliyannis, C. P., Steinhauer, A., & Jeffries, R. D. 2002, *ApJ*, **577**, L39
- Den Hartog, E. A., Ruffoni, M. P., Lawler, J. E., et al. 2014, *ApJS*, **215**, 23
- Denissenkov, P. A. 2012, *ApJ*, **753**, L3
- Duncan, D. K., Vaughan, A. H., Wilson, O. C., et al. 1991, *ApJS*, **76**, 383
- Eberhard, G., & Schwarzschild, K. 1913, *ApJ*, **38**, 292
- Eggleton, P. P., Dearborn, D. S. P., & Lattanzio, J. C. 2006, *Science*, **314**, 1580
- Gonzalez, G., & Vanture, A. D. 1998, *A&A*, **339**, L29
- Ibukiyama, A., & Arimoto, N. 2002, *A&A*, **394**, 927
- Isaacson, H., & Fischer, D. 2010, *ApJ*, **725**, 875
- Johnson, D. R. H., & Soderblom, D. R. 1987, *AJ*, **93**, 864
- Koch, A., Lind, K., Thompson, I. B., & Rich, R. M. 2012, *Mem. Soc. Astron. It. Suppl.*, **22**, 79
- Kumar, Y. B., Reddy, B. E., & Lambert, D. L. 2011, *ApJ*, **730**, L12
- Lawler, J. E., Bonvallet, G., & Sneden, C. 2001a, *ApJ*, **556**, 452
- Lawler, J. E., Wickliffe, M. E., den Hartog, E. A., & Sneden, C. 2001b, *ApJ*, **563**, 1075
- Lawler, J. E., Guzman, A., Wood, M. P., Sneden, C., & Cowan, J. J. 2013, *ApJS*, **205**, 11
- Lebzelter, T., Uttenthaler, S., Busso, M., Schultheis, M., & Aringer, B. 2012, *A&A*, **538**, A36
- Lind, K., Asplund, M., & Barklem, P. S. 2009, *A&A*, **503**, 541
- Liu, Y. J., Tan, K. F., Wang, L., et al. 2014, *ApJ*, **785**, 94
- Luck, R. E., & Heiter, U. 2007, *AJ*, **133**, 2464
- Martell, S. L., & Shetrone, M. D. 2013, *MNRAS*, **430**, 611
- Meléndez, J., & Barbuy, B. 2009, *A&A*, **497**, 611
- Mermilliod, J.-C. 1986, *Catalogue of Eggen's UB data*
- Monaco, L., Villanova, S., Bonifacio, P., et al. 2012, *A&A*, **539**, A157
- Monaco, L., Boffin, H. M. J., Bonifacio, P., et al. 2014, *A&A*, **564**, L6
- Niedzielski, A., Villaver, E., Wolszczan, A., et al. 2015, *A&A*, **573**, A36
- Nowak, G. 2012, Ph.D. Thesis, UMK Toruń
- Nowak, G., Niedzielski, A., Wolszczan, A., Adamów, M., & Maciejewski, G. 2013, *ApJ*, **770**, 53
- O'Brian, T. R., Wickliffe, M. E., Lawler, J. E., Whaling, W., & Brault, J. W. 1991, *J. Opt. Soc. Am. B Opt. Phys.*, **8**, 1185
- Pasquini, L., Koch, A., Smiljanic, R., Bonifacio, P., & Modigliani, A. 2014, *A&A*, **563**, A3
- Pilachowski, C., Saha, A., & Hobbs, L. M. 1988, *PASP*, **100**, 474
- Pilachowski, C. A., Sneden, C., Kraft, R. P., Harmer, D., & Willmarth, D. 2000, *AJ*, **119**, 2895
- Plez, B., & Cohen, J. G. 2005, *A&A*, **434**, 1117
- Ram, R. S., Brooke, J. S. A., Bernath, P. F., Sneden, C., & Lucatello, S. 2014, *ApJS*, **211**, 5
- Ramírez, I., & Allende Prieto, C. 2011, *ApJ*, **743**, 135
- Ramírez, I., & Meléndez, J. 2005, *ApJ*, **626**, 465
- Ramsey, L. W., Adams, M. T., Barnes, T. G., et al. 1998, in SPIE Conf. Ser. 3352, ed. L. M. Stepp, 34
- Raskin, G., van Winckel, H., Hensberge, H., et al. 2011, *A&A*, **526**, A69
- Reddy, B. E., & Lambert, D. L. 2005, *AJ*, **129**, 2831
- Reddy, B. E., Lambert, D. L., Hrivnak, B. J., & Bakker, E. J. 2002, *AJ*, **123**, 1993
- Ruchti, G. R., Fulbright, J. P., Wyse, R. F. G., et al. 2011, *ApJ*, **743**, 107
- Ruffoni, M. P., Den Hartog, E. A., Lawler, J. E., et al. 2014, *MNRAS*, **441**, 3127
- Sackmann, I.-J., & Boothroyd, A. I. 1999, *ApJ*, **510**, 217
- Shetrone, M., Cornell, M. E., Fowler, J. R., et al. 2007, *PASP*, **119**, 556
- Siess, L., & Livio, M. 1999, *MNRAS*, **308**, 1133
- Sneden, C. 1973, *ApJ*, **184**, 839
- Sneden, C., Lucatello, S., Ram, R. S., Brooke, J. S. A., & Bernath, P. 2014, *ApJS*, **214**, 26
- Sousa, S. G., Santos, N. C., Israelian, G., Mayor, M., & Monteiro, M. J. P. F. G. 2007, *A&A*, **469**, 783
- Sweigart, A. V., Greggio, L., & Renzini, A. 1989, *ApJS*, **69**, 911
- Takeda, Y., Sato, B., Kambe, E., et al. 2005, *PASJ*, **57**, 109
- Terasawa, M., Sumiyoshi, K., Kajino, T., Mathews, G. J., & Tanihata, I. 2001, *ApJ*, **562**, 470
- Tull, R. G. 1998, in SPIE Conf. Ser. 3355, ed. S. D'Odorico, 387
- Valenti, J. A., & Piskunov, N. 1996, *A&AS*, **118**, 595
- van Leeuwen, F. 2007, *A&A*, **474**, 653
- Villaver, E., & Livio, M. 2009, *ApJ*, **705**, L81
- Villaver, E., Livio, M., Mustill, A. J., & Siess, L. 2014, *ApJ*, **794**, 3
- Wilson, R. E. 1953, *General Catalogue of Stellar Radial Velocities* (Carnegie Institute Washington D.C. Publication)
- Wood, M. P., Lawler, J. E., Sneden, C., & Cowan, J. J. 2013, *ApJS*, **208**, 27
- Woosley, S. E., & Weaver, T. A. 1995, *ApJS*, **101**, 181
- Wright, E. L., Eisenhardt, P. R. M., Mainzer, A. K., et al. 2010, *AJ*, **140**, 1868